0026-895X/06/7004-1271–1280$20.00
MOLECULAR PHARMACOLOGY

Mol Pharmacol 70:1271–1280, 2006

Vol. 70, No. 4
26567/3144187
Printed in U.S.A.

On the Mechanism of Action of 9-*O*-Arylalkyloxime Derivatives of 6-*O*-Mycaminosyltylonolide, a New Class of 16-Membered Macrolide Antibiotics[S]

Panagiotis Karahalios, Dimitrios L. Kalpaxis, Hong Fu, Leonard Katz, Daniel N. Wilson, and George P. Dinos

Laboratory of Biochemistry, School of Medicine, University of Patras, Patras, Greece (P.K., D.L.K., G.P.D); Kosan Biosciences Inc., Hayward, California (H.F., L.K.); Max-Planck-Institute für Molekulare Genetik, AG Ribosomen, Berlin, Germany (D.N.W.)

Received May 11, 2006; accepted July 27, 2006

ABSTRACT

New 16-membered 9-aryl-alkyl oxime derivatives of 5-*O*-mycaminosyl-tylonolid (OMT) have recently been prepared and were found to exhibit high activity against macrolide-resistant strains. In this study, we show that these compounds do not affect the binding of tRNAs to ribosomes in a cell-free system derived from *Escherichia coli* and that they cannot inhibit peptidyltransferase, peptidyl-tRNA translocation, or poly(U)-dependent poly(Phe) synthesis. However, they severely inhibit poly(A)-dependent poly(Lys) synthesis and compete with erythromycin or tylosin for binding to common or partially overlapping sites in the ribosome. According to footprinting analysis, the lactone ring of these compounds seems to occupy the classic binding site of macrolides that is located at the entrance of the exit tunnel, whereas the extending alkyl-aryl side chain seems to penetrate deeper in the tunnel, where it protects nucleoside A752 in domain II of 23S rRNA. In addition, this side chain causes an increased affinity for mutant ribosomes that may be responsible for their effectiveness against macrolide resistant strains. As revealed by detailed kinetic analysis, these compounds behave as slow-binding ligands interacting with functional ribosomal complexes through a one-step mechanism. This type of inhibitor has several attractive features and offers many chances in designing new potent drugs.

The ribosome and translation are major cellular targets of antibiotics (reviewed by Hermann, 2005). The macrolide class of antibiotics represents a large family of clinical important antimicrobial agents that inhibit protein synthesis by binding to the ribosome (Omura, 2002). Each family member is characterized by the presence of a lactone ring that varies in size and to which distinctive side-chain moieties are attached (Fig. 1). Like the 14-membered macrolides, 16-membered macrolides are active mainly against Gram-positive bacteria and *Mycoplasma* species. They show some advantages over 14-membered macrolides, having better gastrointestinal tolerance and activity against strains expressing resistance of the inducible type (Katz and Ashley, 2005). Even as early as the 1960s, efforts were initiated to synthesize macrolide derivatives with improved activity to combat the emerging presence of drug-resistant bacteria. Today, several series of 14-membered macrolides belonging to the ketolide class, derived from erythromycin, exhibit useful antimicrobial activity against various resistant strains (Ackermann and Rodloff, 2003). These ketolides are believed to overcome macrolide resistance in *Streptococcus pneumoniae* and *Streptococcus pyogenes* through enhanced binding to the bacterial ribosome via their aromatic side chains and to better evade the efflux systems. Similar developments have recently been made with the 16-membered macrolides. Using 5-*O*-mycaminosyltylonolid (OMT), a precursor in the biosynthesis of the macrolide tylosin as the starting compound, an alkylaryl group was introduced at the C9 position of the lactone ring with linkers of varying length (Fu et al., 2005). According to the reported MIC values, two of the new derivatives exhibited superior activity against both macrolide-susceptible and macrolide-resistant strains. It is noteworthy that the compounds, termed C-1 and C-2, each have a side-chain linker length of four atoms, as shown in Fig. 1.

Because these compounds are promising as potent new antibacterial agents, we were interested in characterizing

This work was supported by Kosan Biosciences Inc. (Hayward, CA).

Article, publication date, and citation information can be found at http://molpharm.aspetjournals.org.

doi:10.1124/mol.106.026567.

[S] The online version of this article (available at http://molpharm.aspetjournals.org) contains supplemental material.

ABBREVIATIONS: OMT, 5-*O*-mycaminosyltylonolid; DMS, dimethylsulfate; EF-G, elongation factor G; PTF, peptidyltransferase; C-1, compound 1; C-2, compound 2; PTF, peptidyltransferase.

their mechanism of action on the ribosome. With this aim, we performed an extensive analysis of the effects of these compounds on specific steps of translation, using a cell-free system derived from *Escherichia coli*. That is to say, we studied their effects on 1) poly(Phe) and poly(Lys) synthesis, 2) binding of tRNAs to the ribosomal A, P, and E sites, 3) peptidyltransferase (PTF) activity of the ribosome, 4) EF-G dependent translocation of tRNAs, 5) binding of the macrolides erythromycin and tylosin to both wild type and A2058G macrolide resistant ribosomes, as well as 6) the susceptibility of 23S rRNA nucleosides to chemical modification by dimethylsulfate (DMS). We found that the OMT compounds 1) bind within the ribosomal tunnel of *Escherichia coli* ribosomes in a partially overlapping and mutually exclusive site with erythromycin and tylosin and 2) form a tight complex, acting as slow binding inhibitors.

Materials and Methods

Materials. Puromycin dihydrochloride (disodium salt), tylosin, erythromycin, GTP, ATP, and tRNA from *E. coli* strain W were purchased from Sigma (St. Louis, MO). Poly(U) and Poly(A) were purchased from Fluka (Buchs, Switzerland). L-[2,3,4,5,6-^{3}H]Phenylalanine, L-[^{14}C]phenylalanine, L-[^{14}C]valine, L-[*methyl*-^{3}H]methionine, L-[^{3}H]lysine, and [γ-^{32}P]ATP were obtained from GE Healthcare (Little Chalfont, Buckinghamshire, UK). [^{14}C]Erythromycin was purchased by Moravek Biochemicals (Brea, CA). Avian myeloblastosis virus reverse transcriptase was purchased from Roche Diagnostics (Mannheim, Germany). Cellulose nitrate filters (type HA; 24-mm diameter, 0.45-μm pore size) were obtained from Millipore Corporation (Bedford, MA). Glass fiber filters were obtained from Schleicher & Schüll (Dassel, Germany).

The 16-membered macrolide scaffold OMT was prepared as described previously by Gorman and Morin (1969), and its 9-*O*-arylalkyloxime derivatives were prepared as described recently (Fu et al., 2005). In brief, the procedure involves the conversion of the 5-*O*-mycaminosyltylonolide C-9 ketone to the corresponding oxime, and then the selective alkylation on the oxygen with the appropriate arylalkylbromides.

Biochemical Preperations. 70S ribosomes, either tight or reassociated, were prepared from *E. coli* K-12 cells as described by Blaha et al. (2000) and were kept in buffer containing 20 mM HEPES/KOH, pH 7.6, 50 mM CH_3COONH_4, 6 mM $(CH_3COO)_2Mg$, and 4 mM β-mercaptoethanol. Following the same procedure, we isolated ribosomes from a strain carrying plasmid pSTL102 (Triman et al., 1989) kindly provided by Alexander Mankin (College of Pharmacy, Chicago, IL). The pSTL102 plasmid carries two mutations. The first, A2058G, is located in the 23S rRNA and confers macrolide resistance, whereas the second, C1192U, is in the 16S rRNA and does not influence macrolide binding. The S-100 fraction was prepared as described by Rheinberger et al. (1988) and was treated with DE-52 cellulose to absorb away the tRNAs and most RNases. MF-mRNA (encoding fMet-Phe) and MVF-mRNA (encoding fMet-Val-Phe) were prepared by run-off transcription as described by Schaefer et al. (2002). Elongation factor EF-G was isolated from *E. coli* as described by Boon et al. (1992). f[^{3}H]Met-tRNA, Ac[^{14}C]Val-tRNA and Ac[^{14}C]Phe-tRNA were prepared using specific tRNAs under standard conditions (Rheinberger et al., 1988) and were freed of uncharged tRNA by reversed-phase HPLC on Nucleosil columns.

Preparation of Defined Ribosomal Complexes. All complexes were prepared under identical ionic conditions: 20 mM HEPES-KOH, pH 7.6, 4.5 mM magnesium acetate, 150 mM ammonium acetate, 2 mM spermidine, 0.05 mM spermine, and 4 mM β-mercaptoethanol (called buffer A), and were kept constant throughout all the steps of complex formation. Reassociated 70S ribosomes were used at a final concentration of 0.3 μM and were incubated in the presence of the appropriate mRNA (2.0 μM) and the charged tRNA (0.5 μM) at 37°C for 15 min (Blaha et al., 2000), unless otherwise indicated. Binding of tRNA was assessed by nitrocellulose filtration, and the puromycin reaction was used to titrate the binding sites (Blaha et al., 2000). Each determination was performed in triplicate with a deviation from the average of less than ±10%.

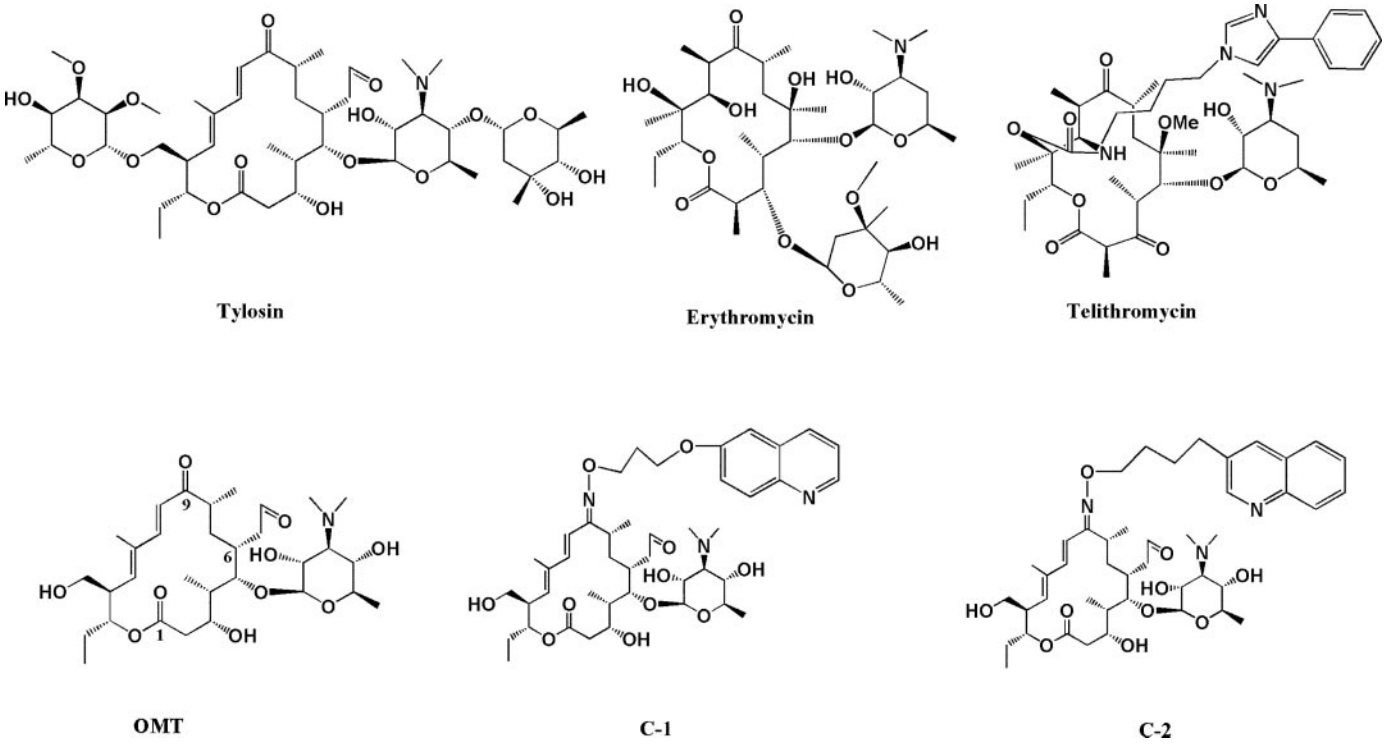

Fig. 1. Chemical structure of tylosin, erythromycin, telithromycin, OMT, C-1, and C-2.

Pi Complex Formation. 70S reassociated ribosomes were incubated in the presence of MF-mRNA or MVF-mRNA with charged tRNA (f[^{3}H]Met-tRNA, Ac[^{3}H]Phe-tRNA, or Ac[^{14}C]Val-tRNA) at 37°C for 15 min.

A-Site Binding and Formation of Pre-Translocation Complexes. 70S ribosomes (0.3 μM) were first incubated with MF or MVF-mRNA and 0.5 μM tRNA^{fMet} (deacylated tRNA) at 37°C for 15 min, to prefill the P site. Next, A-site binding was performed by addition of Ac[^{14}C]Phe-tRNA or Ac[^{14}C]Val-tRNA (0.5 μM), and incubation was continued for 30 min at 37°C. Titration with puromycin (1 mM, 2 min, 37°C) gave no product, indicating that all bound peptidyl-tRNA was exclusively bound to the A site.

Post-Translocation Complexes. After formation of pretranslocation complexes (as described previously), EF-G (0.3 pmol of EF-G/pmol of 70S) and GTP (final concentration, 0.4 mM) were added and the incubation continued for 15 min at 37°C. The puromycin reaction titrated the new state of the ribosome. In each case, the ribosome-bound fraction of tRNAs was calculated by nitrocellulose filtration. A small volume of the incubation mixture was mixed with 2 ml of ice-cold buffer A, passed immediately through cellulose nitrate filters, and washed twice with 2 ml of ice-cold buffer A. The radioactivity remaining on the filter was determined by liquid scintillation.

Puromycin Reaction. Reactions between defined ribosomal complexes and excess of puromycin were carried out at 37°C for 2 min. In general, the reaction volume was 20 μl, and puromycin (in buffer A) was added to a final concentration of 1 mM. After incubation, the reaction was stopped by the addition of an equal volume of 0.3 M sodium acetate, pH 5.5, saturated with $MgSO_4$. Extraction with 1 ml of ethyl acetate followed, and the radioactivity contained in 700 μl of the organic phase was determined by liquid scintillation counting. Beyond titrating the tRNA binding sites, puromycin was also used to estimate the PTF activity (see *Results*).

Poly(U)-Dependent Poly(Phe) Synthesis. The assay was carried out in buffer A with tight-coupled 70S ribosomes and was performed in reaction volumes of 15 μl. Each incubation mixture contained 70S ribosomes (0.20 μM) preincubated with each antibiotic for 10 min at 37°C, fractionated poly(U) (25 μg), [^{3}H]phenylalanine (5 nmol, 50 dpm/pmol), bulk tRNA from *E. coli* (1 A_{260} unit), ATP (3 mM), GTP (1.5 mM), acetyl phosphate (5 mM), and S-100 fraction. After 60-min incubation at 37°C, hot trichloroacetic acid precipitation followed, and polypeptides were isolated on glass fiber filters (Bommer et al., 1996). The remaining radioactivity on the filters was measured in a liquid scintillation counter. To check the response of the applied translation system, a strong inhibitor of poly(Phe) synthesis, edeine, was also used at 50 μM concentration.

Poly(A)-Dependent Poly(Lys) Synthesis. This assay was performed as described for poly(Phe) synthesis, except that the poly(A) replaced poly(U) and [^{3}H]lysine (3 nmol, 500 dpm/pmol) replaced phenylalanine. The trichloroacetic acid solution used for polylysine peptides precipitation was treated with 0.25% sodium tungstate before use. The incubation took place at 37°C for 1 h.

Competition of [^{14}C]Erythromycin Binding. 70S tight-coupled ribosomes (0.20 μM) in buffer A were incubated with [^{14}C]erythromycin (200 dpm/pmol) in the appropriate concentration. After incubation for 10 min at 37°C, the mixture was diluted with 3 ml of ice-cold buffer A and was filtered through a cellulose nitrate filter. The tube and filter were immediately washed an additional two times with 3 ml of ice-cold buffer A and the absorbed radioactivity was determined by liquid scintillation counting. Next, the bound radioactivity was measured by adding a constant [^{14}C]erythromycin concentration (0.6 μM) and increasing concentration of nonradioactive compounds, either erythromycin or one of the new macrolides to compete the bound radioactivity and to occupy its binding site.

Inactivation of Complex C by Tylosin in the Absence or Presence of Macrolides. Pi complex was prepared as described above and absorbed on a cellulose nitrate filter (called complex C). Then, the filter was immersed in buffer A containing either constant tylosin and increasing concentration of each one of the new macrolides or a constant concentration of new macrolide and increasing tylosin concentrations. The exposure of complex C took place at 25°C, either as a time course to follow the progress of the reactions, or for 10 min, enough time for the system to reach equilibrium. To stop the reaction, each filter was immersed in 15 ml of ice-cold buffer A and then washed three times with the same buffer to remove traces of nonspecifically bound tylosin. The remaining activity of complex C was determined by titration with 2 mM puromycin for 2 min at 25°C (Dinos and Kalpaxis 2000). All data illustrated in the figures denote the mean values obtained from four independently performed experiments.

Antibiotic Probing and Chemical Modification. Aliquots of *E. coli* 70S ribosomes, 50 pmol per tube, were initially activated for 5 min at 37°C in buffer containing 20 mM HEPES/KOH, pH 7.8, 20 mM $MgCl_2$, and 300 mM KCl. Next, antibiotics were added in the appropriate concentration up to the final volume of 100 μl in the same buffer, and the reaction mixtures were incubated for 10 min at 37°C. After cooling on ice, chemical modification of ribosomes was carried out by adding 5 μl of DMS (diluted 1:5 in ethanol) and incubating for 10 min at 37°C. The DMS reactions were stopped by the addition of 25 μl of stop solution (1 M Tris/HCl, pH 7.5, 1 M β-mercaptoethanol, and 0.1 mM EDTA). Next, the ribosomes were ethanol-precipitated, and the pellets were resuspended in 50 μl of buffer containing 10 mM Tris/HCl, pH 7.5, 100 mM NH_4Cl, 5 mM EDTA, and 0.5% SDS. Ribosomal RNA was isolated by extraction with equal volumes of phenol, phenol-chloroform, and chloroform, followed by ethanol precipitation. Finally, rRNA was resuspended in water.

Primer Extension. The modifications in 23S rRNA were monitored by primer extension analysis using avian myeloblastosis virus-reverse transcriptase and 5′-labeled primers. We used two primers, one complementary to nucleotides 2141 to 2157 and the other complementary to 816 to 835. The cDNA products of the primer extension reactions were separated by electrophoresis on 6% polyacrylamide sequencing gels. Gels were scanned and analyzed by PhosphorImager (GE Healthcare) before classic autoradiography on X-ray films. The positions of the stops in cDNA synthesis were identified by reference to dideoxy sequencing reactions on 23S rRNA, run in parallel (Stern et al., 1988). The experiments were repeated up to four times.

Results

The 16-Membered Arylalkyl Oxime Macrolides Severely Inhibited Poly(A)-Dependent Poly(Lys) Synthesis, but Not Poly(U)-Dependent Poly(Phe) Synthesis. Because poly(Phe) formation has been previously shown to exhibit "immunity" to the inhibitory effect of 14-membered macrolide antibiotics but not to 16-membered (Omura, 2002), we were interested in determining whether this observation also held in the presence of OMT-derivatives. To test this, we performed poly(U)-dependent poly(Phe) synthesis in the presence of the parent compound OMT or its derivatives compound 1 (C-1) and compound 2 (C-2). For comparison, we included also erythromycin and tylosin. As a positive control, we included edeine. As shown in Fig. 2A, OMT and its derivatives, at concentrations up to 20 μM, failed to inhibit poly(Phe) synthesis. As expected, erythromycin was also ineffective, whereas tylosin and edeine were strong inhibitors. However, the three 16-membered macrolides were found to be effective inhibitors of poly(Lys) synthesis. As shown in Fig. 2B, the level of inhibition caused by the three inhibitors, each one used at 2 μM, was similar to that obtained with 50 μM edeine, 2 μM tylosin, or 2 μM erythromycin. The inset in Fig. 2B illustrates the effect of increasing C-1 concentration on poly(Lys) formation. According to this plot, an inhibition

plateau was reached at concentrations approaching 2 μM. The IC_{50} [concentration of the drug at which 50% inhibition of poly(Lys) synthesis is achieved] was estimated to be approximately 0.5 μM, a value comparable with that found for erythromycin and tylosin (data not shown). From similar inhibitory curves (data not shown), the IC_{50} values for OMT and C-2 were found to be 0.45 and 0.48 μM, respectively.

Effect of OMT-Derivatives on tRNA Binding, Peptide-Bond Formation, and Peptidyl-tRNA Translocation. According to the above in vitro translation data, OMT and its derivatives displayed inhibitory features typical of classic macrolides; i.e., they inhibited poly(Lys) but not poly(Phe) synthesis. It is also known that the growing poly(Lys) chain follows the physiological exit route, passing across the exit tunnel, in contrast to a poly(Phe) chain, which does not enter into the tunnel (Picking et al., 1991). Therefore, it is reasonable to suggest that OMT and its derivatives inhibited translation by hindering the transit of the growing polypeptide chain through the exit tunnel. Nevertheless, additional effects of the new 16-membered macrolides on other steps of translation process cannot be a priori excluded. Therefore, we designed a series of experiments to reveal possible effects of 16-membered macrolides on: 1) binding of Ac-[^{14}C]Val-tRNA and f[^{3}H]Met-tRNA to the P site of MVF-mRNA programmed ribosomes, 2) binding of Ac-[^{14}C]Val-tRNA to the A site of MVF-programmed ribosomes, and 3) binding of uncharged $tRNA^{fMet}$ to the P and E sites of the MVF-mRNA programmed ribosomes. We observed no inhibition in tRNA binding at any one of these tests, even by using excessively high concentrations of antibiotics (20 μM, data not shown). Next, we checked for possible effects on PTF activity. In these assays, MF-mRNA programmed ribosomes carrying Ac[^{14}C]Phe-tRNA at the P site (Pi complex) were reacted with puromycin in the presence of antibiotics. No inhibition in AcPhe-puromycin formation by OMT or its derivatives was observed, whereas clear inhibition by tylosin and spiramycin was detected (Fig. 2C). PRE-complexes were then prepared, using reassociated 70S ribosomes programmed with MVF-mRNA and carrying $tRNA^{fMet}$ in the P site and Ac[^{14}C]Val-tRNA in the A site. As shown in Fig. 2D, efficient binding of Ac[^{14}C]Val-tRNA to the A site was achieved (0.8 tRNA/ribosome, black bar). Figure 2D shows also that when EF-G is absent, titration with puromycin gave almost no product (gray bar), a fact indicating that Ac[^{14}C]Val-tRNA is present exclusively at the A site. However, in the presence of EF-G and GTP, the puromycin reac-

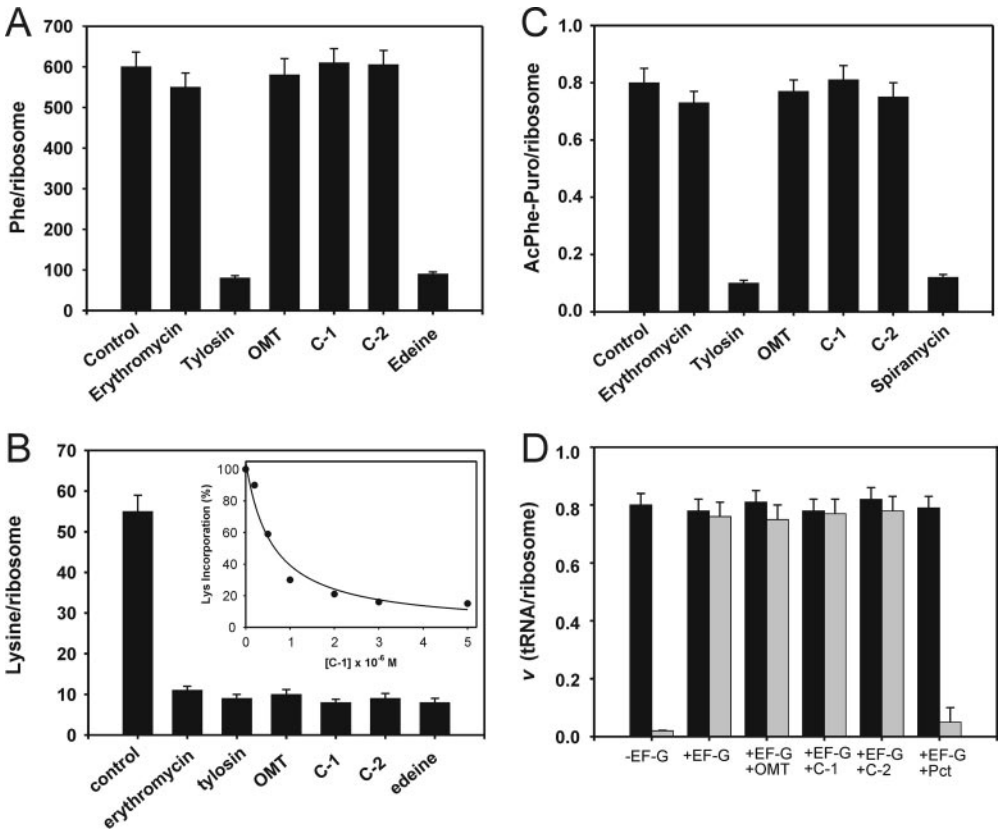

Fig. 2. Effect of OMT and its alkyl-aryl-derivatives on poly(Phe) synthesis, poly(Lys) synthesis, puromycin reaction, and translocation. A, poly(Phe) synthesis in the absence or in the presence of erythromycin, tylosin, OMT, C-1, C-2, and edeine. The concentration of each antibiotic was 20 μM (except edeine, at 50 μM), and the reaction mixture was incubated at 37°C for 60 min. B, poly(Lys) synthesis in the absence or in the presence of erythromycin, tylosin, OMT, C-1, C-2, and edeine. Experimental conditions and antibiotic concentration are the same as before. The inset plot shows poly(Lys) synthesis as a function of C-1 concentration. 100% is equivalent to 54 Lys/ribosome, observed in the absence of antibiotic after 60-min incubation at 37°C. C, puromycin reaction in the absence or in the presence (2 μM) of erythromycin, tylosin, OMT, C-1, C-2, and spiramycin. In these assays, Pi ribosomal complex containing Ac[^{14}C]Phe-tRNA at the P site of MF-mRNA programmed 70S ribosomes was reacted with 1 mM puromycin at 37°C for 2 min. D, effect of OMT and its alkyl-aryl-derivatives on A-site binding and translocation of tRNA. Ac[^{14}C]Val-tRNA was bound to the A site (black bars) of MVF-mRNA programmed 70S ribosomes bearing $tRNA^{fMet}$ at the P site. The prepared PRE-complex was incubated in the presence or in the absence of EF-G and GTP (37°C, 15 min), and then titration was followed with puromycin (gray bars). The same reaction was also carried out in the presence of 10 μM of OMT, C-1, and C-2. In the last two bars, the assay took place in the presence of 10 μM pactamycin, a strong inhibitor of translocation (positive control).

tion is almost quantitative (0.78 pmol of Ac[^{14}C]Val-puromycin formed per ribosome), a fact indicating successful translocation of the donor Ac[^{14}C]Val-tRNA from the A to the P site. Identical results were obtained in the presence of 10 μM OMT, C-1, or C-2 compounds (Fig. 2D), suggesting that these compounds exerted no inhibitory effect on translocation. As expected, in the presence of 10 μM pactamycin, an effective translocation inhibitor (Dinos et al., 2004), translocation was totally abolished. The PTF activity was also tested with the puromycin reaction in the presence of the antibiotics using one additional complex, namely ribosomes carrying f[^{3}H]Met-tRNA in the P site of 70S ribosomes programmed with MF-mRNA. In addition, in this case, there was no inhibition in fMet-puromycin formation by any one of the new 16-membered macrolides (data not shown).

Competition Binding Studies. The binding of [^{14}C]erythromycin to ribosomes was studied in the presence of ribosomes at constant concentration and increasing radioactive erythromycin concentrations. The data were analyzed by a Scatchard plot (data not shown), which gave a dissociation constant (K'_D) for erythromycin equal to 15 $\pm$ 2 nM, in agreement with values reported earlier (Pestka and Lemahieu, 1974; Lovmar et al., 2004). Next, the competition of [^{14}C]erythromycin binding by nonradioactive erythromycin or by each one of the 16-membered macrolides was determined. As shown in Fig. 3A, the saturation ratio ν (picomoles of bound [^{14}C]erythromycin per picomole of ribosomes) decreases with increasing concentrations of nonradioactive erythromycin or C-1. At high concentrations of C-1, this ratio approaches zero. This means that C-1 binds at a position mutually exclusive with the erythromycin binding site. Analogous plots were obtained with OMT or C-2 (not shown). The dissociation constant (K_D) for each antibiotic was evaluated from plots of $1/\nu$ versus [A], where [A] is the concentration of the competing ligand (Fig. 3B). $1/\nu$ is related to [A] by eq. 1

$$\frac{1}{\nu} = \frac{[E] + K_D}{[E]} + \frac{K'_D}{K_D}[A] \quad (1)$$

where K'_D is the dissociation constant of erythromycin binding to ribosomes, and [E] is the concentration of radioactive erythromycin. The K_D values calculated from the slopes of these plots are presented in Table 1.

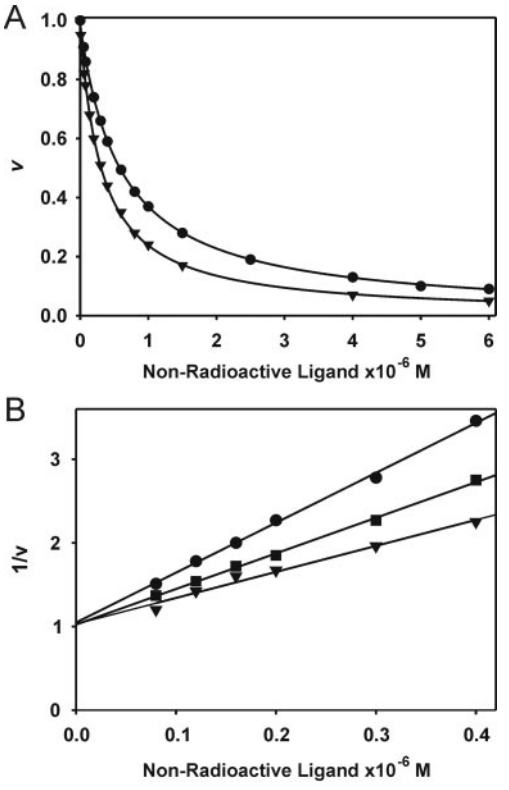

Fig. 3. Competition of the [^{14}C]erythromycin binding to vacant ribosomes by nonradioactive erythromycin or 16-membered new macrolides. A, plot of ν (picomoles of bound [^{14}C]erythromycin per picomole of ribosomes) versus the concentration of C-1 (▼) or nonradioactive erythromycin (●). The concentration of ribosomes was multiplied by 0.7, a factor that represents the active fraction of tight ribosomes capable for binding erythromycin. B, plot of $1/\nu$ versus the concentration of OMT (●), C-1 (▼), and C-2 (■).

Inactivation of Complex C by Tylosin in the Presence of Macrolides. The conventional assay to estimate the activity status of PTF activity is the puromycin reaction. This reaction is a model assay system for testing PTF activity and takes place according to the kinetic Scheme 1. In the presence of excess puromycin, the reaction follows pseudo-first-order kinetics and the relationship

$$ln\frac{C_0}{C_0 - P} = k_{obs} \times t \quad (2)$$

holds; C_0 is the reactive complex C at zero time expressed as percentage of the total radioactivity isolated on the filter disc, and k_{obs} is the apparent rate constant of product formation. Representative semilogarithmic time plots of the puromycin reaction carried out in the presence or in the absence of antibiotics, are given in Fig. 4A. The linearity of the plots obtained when the reaction took place either in the absence or in the presence of OMT, C-1, and C-2, not only agreed with eq. 2 but also confirmed that these novel 16-membered macrolides did not inhibit the PTF activity. In contrast, in the presence of tylosin, the progress curve deviates from linearity and, as we have demonstrated previously (Dinos and Kalpaxis, 2000), after 2 min reaches a plateau. In the simultaneous presence of 0.5 μM C-1, the inhibitory effect became lower; finally, at high C-1 concentrations, the inhibition was totally abolished (Fig. 4A). OMT and C-2 exert similar ability

TABLE 1

Dissociation constants of 70S ribosomal complexes with macrolides

The value for erythromycin was estimated by Scatchard-plot analysis, and the values for OMT, C-1, and C-2 were estimated by binding studies, where each one of the indicated antibiotics competed with [^{14}C]erythromycin for binding to vacant 70S ribosomes.

Antibiotic	Dissociation Constant (K_D)
	nM
Erythromycin	15.00 $\pm$ 2.00
OMT	4.19 $\pm$ 0.56
C-1	8.07 $\pm$ 1.08
C-2	5.87 $\pm$ 0.79

$$C + S \underset{}{\overset{K_s}{\rightleftharpoons}} CS \xrightarrow{k_3} C' + P$$

Scheme 1. Kinetic model of puromycin reaction. C is the Pi ribosomal complex free of excess of donor, S is the acceptor substrate puromycin, P is the product Ac[^{3}H]Phe-puromycin, and C′ is the complex C without bound donor Ac[^{3}H]Phe-tRNA at the P site, rendering it unable to react in a second cycle with puromycin.

to relieve the inactivation of complex by tylosin. These results are reminiscent of previous observations (Dinos and Kalpaxis, 2000; Dinos et al., 2003), according to which complex C exposed to tylosin and a competitor not inhibiting the PTF activity (e.g., erythromycin or clarithromycin) exhibits higher reactivity against puromycin than that measured in the presence of tylosin alone. In conclusion, although not inhibiting puromycin reaction, the three 16-membered macrolides compete with tylosin for binding to ribosomes. In theory, this type of competition can follow two alternative mechanisms, depicted in Schemes 2 and 3. Symbols I, A, and C represent tylosin, a new 16-membered macrolide, and the Pi ribosomal complex, respectively. Derivation of the kinetic equations concerning Scheme 3 is given in detail in the Supplementary Material, whereas kinetic equations standing for Scheme 2 have been presented elsewhere (Dinos and Kalpaxis, 2000). Processing our data according to Schemes 2 and 3, we realized that data analysis fit better with Scheme 3. For instance, the plots shown in Fig. 4, B and C, are linear, a fact supporting the validity of Scheme 3. Furthermore, these plots allow us to calculate the kinetic parameters involved in Scheme 3. According to eq. S7 in Supplementary Material, the k_6 value can be estimated from the slope of $1/(C*I)_\infty$ versus [A] plots. Plotting $1/(C*I)_\infty$ versus 1/[I] for constant [A], we can re-calculate and verify the k_6 value, as eq. S8 in Supplementary Material indicates. The estimated values of k_6 for each of the tested antibiotics are presented in Table 2.

To calculate the k_7 value, complex C*A was prepared by exposing complex C to a solution containing each one of the 16-membered macrolides at high concentration. This complex was adsorbed on a cellulose nitrate filter, washed with buffer, and then exposed to 1 μM tylosin for various time intervals. The inactivation of PTF activity was monitored by the puromycin reaction. During this process, complex C was released from C*A complex through the k_7 step and then, reacting rapidly with tylosin, was converted to the inactive form C*I. Because the k_7 step is the rate-limiting step, the slope of the inactivation curve provides the k_7 value (Fig. 4D). The estimated k_7 values, as well as the k_7/k_6 values describing the overall dissociation constant (K_i), are presented in Table 2. Comparing the dissociation constant values in Tables 1 and 2, we can conclude that they resemble each other, regardless of the method applied.

Footprinting Data. The competition of the new 16-membered macrolides with tylosin and erythromycin for common or partially overlapping binding sites on the ribosome is consistent with the chemical protection of 23S rRNA from DMS modifica-

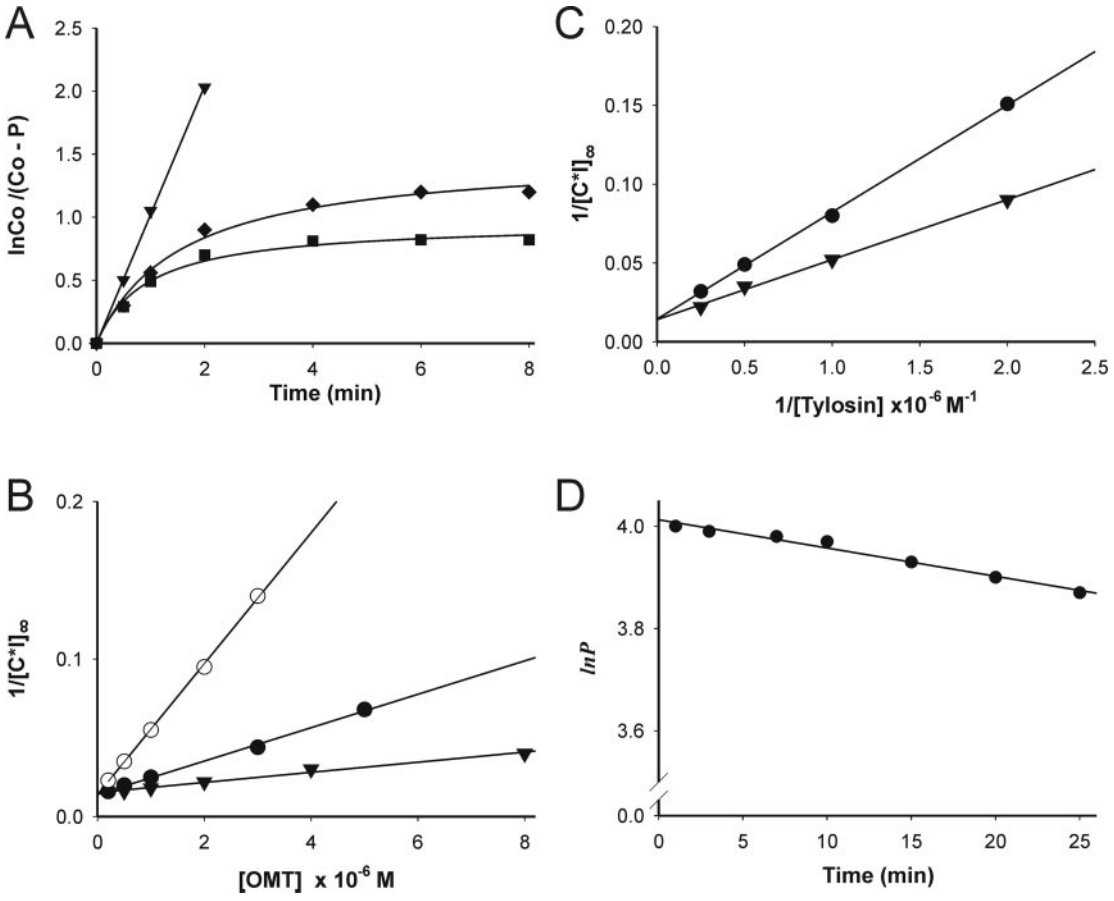

Fig. 4. Kinetic plots for the interaction of 16-membered macrolides with functional ribosomal complexes, in the presence or in the absence of puromycin. A, first-order time plots for AcPhe-puromycin formation in the absence of antibiotic or in the presence of 2 μM concentrations each one of OMT or C-1, or C-2 (▲), 2 μM tylosin (■), and 2 μM tylosin plus 0.5 μM C-1 (♦). The puromycin concentration was 100 μM and the reaction was carried out at 25°C. B, plot of $1/(C*I)_\infty$ versus [OMT]. The reaction mixture contained tylosin at 1 μM (○), 4 μM (●), or 8 μM (▼). C, plot of $1/(C*I)_\infty$ versus 1/[tylosin]. The reaction mixture contained OMT at 1 μM (▼) or 2 μM (●). D, determination of the dissociation rate constant (k_7) of the complex between antibiotic C-1 and ribosomal complex C. Drug-ribosome complex was prepared in the presence of 2 μM C-1 and absorbed on a cellulose nitrate filter. Then, it was exposed to 10 μM tylosin for various time intervals, after which the remaining activity was titrated with puromycin. The k_7 value was estimated from the slope of the linear time plot.

tion. Footprinting analysis in domain V of 23S rRNA revealed that the three antibiotics OMT, C-1, and C-2 (lanes 6–8 in Fig. 5*A*) protect nucleotides A2058 and A2059 from DMS modification similarly to erythromycin, telithromycin, and tylosin (Fig. 5A, lanes 3–5) In addition, strong protection of A752 (Fig. 5B) was observed by C-1 and C-2, suggesting that these antibiotics also influence the susceptibility of nucleotides at the tip of domain II of 23S rRNA, which is located deeper in the ribosomal tunnel. This footprinting pattern is in agreement with the observations of Fu et al. (2005) and confirms the hypothesis that the extending alkyl-aryl arm in the derivatives of OMT causes additional alterations in ribosomal structure, which may be related to the better antimicrobial potency exhibited by these macrolides.

Binding of OMT and OMT-Derivatives to Macrolide Resistant Ribosomes. Until now, little difference in ribosome binding affinity between OMT, C-1, and C-2 has been observed. Yet, C-1 and C-2 are both known to be more effective against macrolide resistant strains than OMT (Fu et al., 2005). This suggested to us that binding of these compounds might deviate when using macrolide resistant ribosomes. To test this, we performed binding experiments using *E. coli* ribosomes bearing A2058G mutations in the 23S rRNA. This mutation confers high-level erythromycin resistance but low-level tylosin resistance (Vester and Douthwaite, 2001). Because of the high-level erythromycin resistance, it was not possible to study binding of the OMT compounds via competition with [^{14}C]erythromycin; the binding of erythromycin was too low (data not shown). However, tylosin still binds efficiently to the mutant ribosomes and, as shown in Fig. 6, at 20 μM final concentration, inactivates complex C by 60%. When complex C was incubated with 5 μM OMT before the addition of tylosin, the inhibition of the puromycin reaction by tylosin remained unchanged, a fact indicating that OMT exhibited low affinity for the mutant ribosomes. As expected, preincubation of complex C with erythromycin also offered no protection against tylosin (Fig. 6). In contrast, preincubation of complex C with 5 μM C-1 or C-2 resulted in a strong protection from the inhibitory effect of tylosin (Fig. 6). In addition, C-1 offered better protection than C-2, indicating that C-1 has a higher affinity for the ribosomal complex than C-2. At higher concentrations (25 μM), both C-1 and C-2 protected completely complex C from tylosin (data not shown). Nevertheless, the fact that tylosin has a lower affinity for complex C than C-1 and C-2 precludes an accurate calculation of the k_{on} and k_{off} values of these compounds.

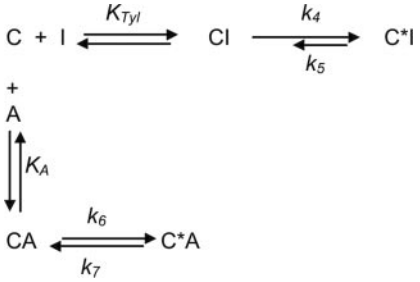

Scheme 2. Two-step mechanism of competition between tylosin (I) and the new 16-membered macrolides (A) for binding on the ribosomal complex C.

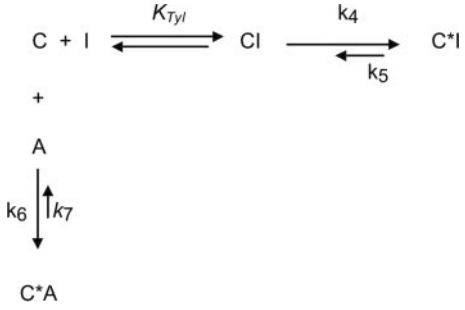

Scheme 3. One-step mechanism of competition between tylosin (I) and the new 16-membered macrolides (A) for binding on the ribosomal complex C.

TABLE 2

Association and dissociation rate constants of 16-membered macrolides with ribosomal complexes

The k_6 values were calculated from kinetic plots similar to those presented in Fig. 4, B and C. The k_7 values were calculated from a dissociation plot similar to that that presented in Fig. 4D. The K_i value was estimated from the ratio k_7/k_6.

Kinetic Constant	Antibiotic		
	OMT	C-1	C-2
$k_6 \times 10^{-4}$ (M^{-1} s^{-1})	2.07 ± 0.35	1.00 ± 0.18	0.40 ± 0.07
$k_7 \times 10^5$ (s^{-1})	9.10 ± 0.66	5.00 ± 0.40	3.33 ± 0.25
K_i (nM)	4.39 ± 0.80	5.00 ± 0.98	8.32 ± 1.58

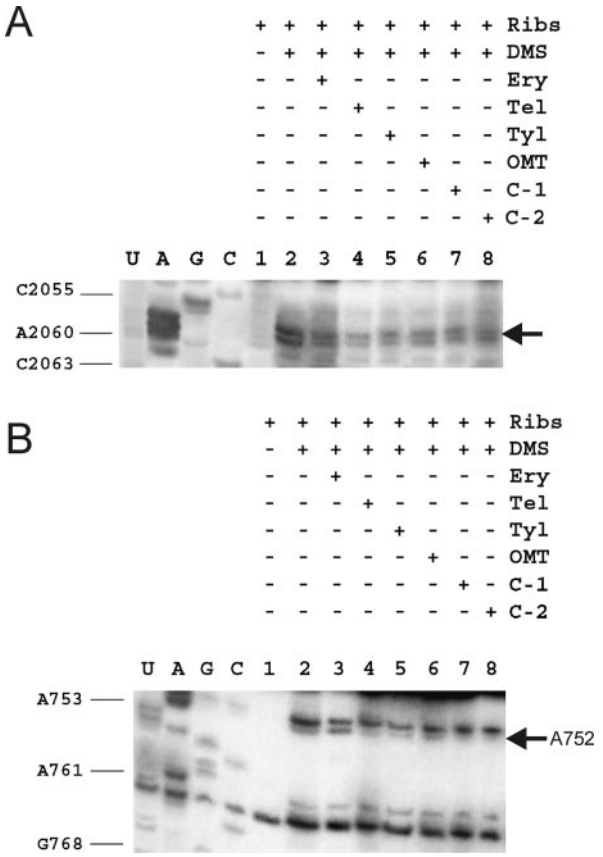

Fig. 5. Protection of 23S rRNA bases from DMS modification by bound antibiotics. A, protection of A2058 and A2059 bases in domain V. Lane 1, untreated 23S rRNA; lane 2, 23S rRNA modified by DMS; lanes 3–8, 23S rRNA preincubated for 10 min at 37°C with erythromycin, telithromycin, tylosin, OMT, C-1, and C-2, respectively, and then modified by DMS. B, protection of A752 base in Helix 35 of domain II. The lanes are numbered as previously. All antibiotics were used at a final concentration equal to 1 μM.

Discussion

Although the tylosin precursor OMT has been known for many years to exhibit high antimicrobial activity (Kirst et al., 1986), the exact mechanism of its interaction with ribosomes had never been studied. In this study, we performed such an analysis, examining the interaction of OMT, as well as the two new OMT derivatives C-1 and C-2, with vacant ribosomes and ribosomal complexes active in peptide bond formation. Such functional studies are important, not only for the establishment of their interaction mode but also to understand the importance and contribution of the inserted aromatic side chains for antimicrobial activity.

According to our data, the new antibiotics behave like classic macrolides. That is to say, they do not inhibit poly(U)-dependent poly(Phe) synthesis (Fig. 2A) but strongly inhibit poly(A)-dependent poly(Lys) synthesis (Fig. 2B). They do not inhibit tRNA binding (at any of the three tRNA binding sites), and they do not inhibit peptidyltransferase (PTF) activity (Fig. 2C). Consistent with other known macrolides, these compounds compete with both 14-membered (erythromycin, Fig. 3) and 16-membered (tylosin, Fig. 4) macrolides for binding to the ribosome and strongly protect the nucleotide bases A2058 and A2059 of 23S rRNA from DMS modification (Fig. 5A). These data support the conclusion that OMT, C-1 and C-2 bind in a position that is at least partially overlapped by the binding site of erythromycin and tylosin. This binding site of macrolide antibiotics on the large ribosomal subunit has been determined by X-ray crystallography to be located in the entrance of the tunnel, adjacent to the PTF center (Schlunzen et al., 2001; Hansen et al., 2002). Therefore, it is tempting to suggest that, by binding to this site, OMT and its derivatives hinder the transit of the growing polypeptide chain through the exit tunnel, a fact that also might cause destabilization of the P site and premature release of peptidyl tRNA. The crystallographic studies also revealed that the mycaminose-mycarose disaccharide hanging from the C5 of the lactone ring of tylosin extends toward the PTF center, explaining the inhibitory effect of tylosin on PTF activity (Dinos and Kalpaxis 2000; current study). The presence of a shorter monosaccharide at the C5 position of OMT, C-1, and C-2 explains why these compounds failed to inhibit the puromycin reaction (Fig. 2C) and, thereafter, poly(U)-dependent phenylalanine incorporation, in contrast to tylosin (Fig. 2A). In addition, by competing off tylosin from the ribosome, they relieved the PTF inhibition associated with the presence of this drug (Fig. 4A).

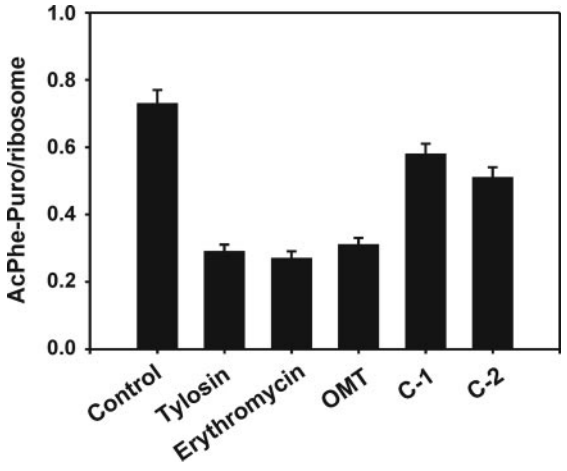

Fig. 6. Puromycin reaction with mutant ribosomes in the absence or in the presence of 20 μM tylosin. Pi ribosomal complex containing Ac[^{14}C]Phe-tRNA at the P site of MF-mRNA programmed 70S ribosomes was first exposed to each antibiotic (final concentration, 5 μM) at 37°C for 2 min, then tylosin was added and incubation proceeded for a further 2 min. Next, the ribosomal complex was reacted with 1 mM puromycin at 37°C for 2 min.

Analysis of the binding position of the macrolide and ketolide antibiotics so far studied in complex with the large ribosomal subunit, has revealed that the lactone ring of these compounds is always positioned similarly, even between archaeal and bacterial ribosomes (Wilson et al., 2005) (Fig. 7). This suggests that the binding of the lactone ring of OMT, C-1, and C-2 is likely to be similar to that of other 16-membered macrolides, such as tylosin. With this assumption, it seems reasonable to assume that the C6-aldehyde group of OMT, C-1, and C-2 will form a covalent bond with the 6-NH_2 of A2062 of the 23S rRNA, as was observed for tylosin (Hansen et al., 2002) and is indicated by an arrow in Fig. 7. Such additional interactions go some way to explain why OMT, C-1, and C-2 have a lower K_D (4–8 nM) than erythromycin (15 nM), which lacks the C6-aldehyde group (Table 1).

As shown in Table 1, the K_D values of C-1 and C-2 are almost equal to that of the parent compound OMT, although their in vivo antimicrobial potencies are markedly superior (Fu et al., 2005). This superior potency can be attributed to several reasons, such as higher drug stability, better intracellular accumulation, and ribosome assembly defects but also to the distinct ability of the alkylaryl side-chains to make additional interactions with the ribosome (Champney, 2003; Katz and Ashley, 2005). Our results are consistent with the latter contribution, because the C-1 and C-2 compounds exhibited an increased affinity for mutant ribosomes compared with OMT (Fig. 6). It remains to be explored whether this increased affinity also holds for other macrolide-resistant ribosomes or ribosomes from other species.

There are many macrolide derivatives with such alkyl-aryl groups in the literature, both 14- and 16-membered, but most prominent among them are the ketolides telithromycin and cethromycin (ABT-773). The binding of these ketolides has been extensively studied with the help of X-ray crystallography. In particular, the binding position of telithromycin has been determined in complex with the *Deinococcus radiodurans* bacterial 50S (D50S) subunits (Berisio et al., 2003; Wilson et al., 2005), as well as *Haloarcula marismortui* archaeal 50S (H50S) subunit (Tu et al., 2005) (Fig. 7). A comparison of the two structures reveals that although the lactone ring of telithromycin binds in an identical fashion to both ribosomes, the alkyl-aryl side chain is quite differently positioned (Wilson et al., 2005). On the H50S, the alkyl-aryl side chain of telithromycin folds back over the lactone ring and stacks on a 23S rRNA base U2609 (Fig. 7) (*E. coli* numbering used throughout). In contrast, in the D50S structure, the alkyl-aryl side chain penetrates deeper into the tunnel where it stacks on base U790 within domain II of the 23S rRNA. Because the equivalent base in the H50S structure is rotated by 180°, such an interaction would not be possible on this archaeal ribosome. Despite the fact that the C-1 and C-2 structures differ from that of telithromycin, the alkyl-aryl side chain attached to these molecules is remarkably similar, and its orientation may be also similar when bound to the ribosome. It should be noted that their C9

position points in the same direction as the telithromycin side chain bound to the D50S, and there is lots of space for arylalkyl side chains to span in this direction (Fig. 7). The strong protection on A752 by C-1 and C-2 (Fig. 5B, lanes 7 and 8) is almost equal to that caused by telithromycin (Xiong et al., 1999) and significantly higher than the protection observed by OMT (Fig. 5B, lane 6). This is in line with the suggestion that the alkyl-aryl side chain of C-1 and C-2 compounds penetrates deeper into the tunnel and establishes additional interactions with nucleotides within domain II of the 23S rRNA. These interactions might play a critical role, particularly if the hydrogen bonding of macrolides with nucleoside A2058 is abolished by mutations or chemical modifications. This fact may explain the increased affinity of the C-1 and C-2 compounds for the mutant ribosomes compared with OMT and erythromycin (Fig. 6).

The association rate constant (k_6) values obtained from the kinetic analysis allow us to classify the three compounds in the large family of the slow binding inhibitors which follow a one-step mechanism of interaction (Morrison and Walsh, 1988). Many studies have demonstrated that macrolides associate slowly with the ribosome, in a time-dependent manner (Di Giambattista et al., 1987; Bertho et al., 1998; Dinos et al., 2003; Lovmar et al., 2004). Controversies between these studies center on the precise mechanism of interaction. Some studies provide support for two-step mechanism (Bertho et al., 1998; Dinos et al., 2003), although there is also evidence for one-step mechanism (Dinos et al., 1993, Lovmar et al., 2004). In fact, a two-step mechanism might be misinterpreted as one-step mechanism if the first step were not easily detectable (Erion and Walsh, 1987). Therefore, we cannot exclude the possibility of an additional rapid weak step in the interaction of 16-membered macrolides with the ribosome, which cannot be detected kinetically under the applied experimental conditions. Compared with OMT, both C-1 and C-2 display a lower dissociation rate constant, a fact that is desirable for newly derived antibiotics, because it results in a longer-lived C∗A complex (Scloss, 1988). On the other hand, both antibiotics show a low association rate constant, which suggests that neither has a ground state complementary to the binding site of the ribosome but might become complementary via an inducible conformational rearrangement. The conformational changes in the ribosome occurring as it exerts its catalytic functions are becoming increasingly in focus (Seo et al., 2006). In addition, the machinery of protein synthesis has evolved as a precise assembly line, with parts constantly in motion and pieces moving through its interior. Thus, the complete picture of macrolide binding and activity is likely to be more complex, perhaps involving transient interactions during the various steps of translation and probably the formation of additional contacts between the antibiotics and the growing nascent peptide chain (Hermann, 2005).

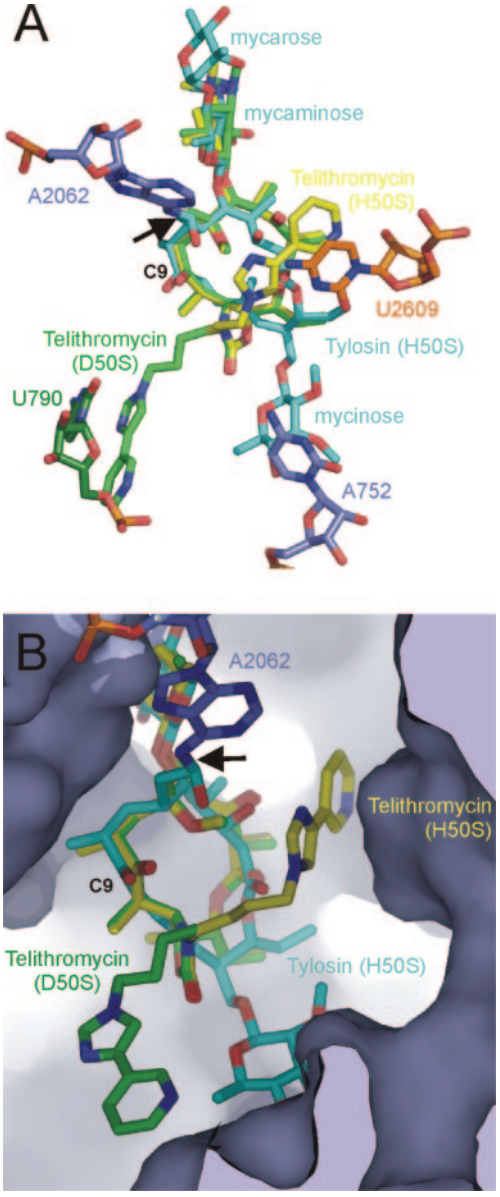

Fig. 7. Relative positions of tylosin and telithromycin on the ribosome. A, alignment of structures of tylosin (cyan) and telithromycin (yellow) bound to the *H. marismortui* large ribosomal subunit (H50S) with telithromycin (green) bound to the *D. radiodurans* large ribosomal subunit (D50S). Features highlighted include the covalent bond between A2062 and the aldehyde of tylosin (indicated also by an arrow), and the C9 carbon of the lactone ring of tylosin to which the arylalkyl side chains are attached for the OMT derivatives. Note that in the H50S, the arylalkyl side chain of telithromycin stacks upon U2609, whereas in the D50S structure, the same side chain penetrates deeper into the tunnel and stacks on U790 within domain II of the 23S rRNA. B, as in A, except illustrating the ribosomal environment of the tunnel with a surface representation. *E. coli* numbering for all bases in both figures is used. This figure uses Protein Data Bank codes 1K9M (tylosin-H50S; Hansen et al., 2002), 1YIJ (telithromycin-H50S; Tu et al., 2005), and telithromycin-D50S from Wilson et al. (2005), and it was created with PyMol (http://www.pymol.org).

Acknowledgments

We thank Dr. Alexander Mankin for kindly providing plasmid pSTL102.

References

Ackermann G and Rodloff AC (2003) Drugs of the 21st century: telithromycin (HMR 3647)-the first ketolide. *J Antimicrob Chemother* **51:**497–511.
Berisio R, Harms J, Schluenzen F, Zarivach R, Hansen HAS, Fucini P, and Yonath A (2003) Structural insight into the antibiotic action of telithromycin against resistant mutants. *J Bacteriol* **185:**4276–4279.
Bertho G, Gharbi-Benarous J, Delaforge M, Lang C, Parent A, and Girault J-P (1998) Conformational analysis of ketolides: conformations of RU004 in solution and bound to bacterial ribosomes. *J Med Chem* **41:**3373–3386.
Blaha G, Stelzl U, Spahn CMT, Agrawal RK, Frank J, and Nierhaus KH (2000) Preparation of functional ribosomal complexes and the effect of buffer conditions on tRNA positions observed by cryoelectron microscopy. *Methods Enzymol* **317:** 292–309.
Bommer U, Burkhardt N, Junemann R, Spahn CMT, Triana-Alonso FJ, and Nierhaus KH (1996) Ribosomes and polysomes, in *Subcellular Fractionation. A Prac-*

tical Approach (J Graham and D Rickwoods eds) pp 271–301, IRL Press at Oxford University Press, Oxford, UK.
Boon K, Vijgenboom E, Madsen LV, Talens A, Kraal B, and Bosch L (1992) Isolation and functional analysis of histidine-tagged elongation factor Tu. *Eur J Biochem* **210:**177–183.
Champney WS (2003) Bacterial ribosomal subunit assembly is an antibiotic target. *Curr Top Med Chem* **3:**929–947.
Di Giambattista M, Engelborghs Y, Nyssen E, and Cocito C (1987) Kinetics of binding of macrolides, lincosamides and synergimycins to ribosomes. *J Biol Chem* **262:**8591–8597.
Dinos G, Synetos D, and Coutsogeorgopoulos C (1993) Interaction between the antibiotic spiramycin and a ribosomal complex active in peptide bond formation. *Biochemistry* **32:**10638–10647.
Dinos GP and Kalpaxis DL (2000) Kinetic studies on the interaction between a ribosomal complex active in peptide bond formation and the macrolide antibiotics tylosin and erythromycin. *Biochemistry* **39:**11621–11628.
Dinos G, Wilson DN, Teraoka Y, Szaflarski W, Fucini P, Kalpaxis D, and Nierhaus KH (2004) Dissecting the ribosomal inhibition mechanisms of edeine and pactamycin: the universally conserved residues G693 and C795 regulate P-site RNA binding. *Mol Cell* **13:**113–124.
Dinos GP, Connell SR, Nierhaus KH, and Kalpaxis DL (2003) Erythromycin, roxithromycin, and clarithromycin: use of slow-binding kinetics to compare their in vitro interaction with a bacterial ribosomal complex active in peptide bond formation. *Mol Pharmacol* **63:**617–623.
Erion MD and Walsh CT (1987) 1-Aminocyclopropanephosphonate: time-dependent inactivation of 1-aminocyclopropanecarboxylate deaminase and *Bacillus stearothermophilus* alanine racemase by slow dissociation behavior. *Biochemistry* **26:**3417–3425.
Fu H, Marquez S, Gu X, Katz L, and Myles DC (2006) Synthesis and in vitro antibiotic activity of 16-membered 9-*O*-arylalkyloxime macrolides. *Bioorg Med Chem Lett* **16:**1259–1266.
Gorman M and Morin RB (1969), inventors; Eli Lilly and Co., assignee. *O*-Mycaminosyl tylomolide and a process for the preparation thereof. U.S. patent 3,459,853. 1969 Aug 5.
Hansen JL, Ippolito JA, Ban N, Nissen P, Moore PB, and Steitz TA (2002) The structures of four macrolide antibiotics bound to the large ribosomal subunit. *Mol Cell* **10:**117–128.
Hermann T (2005) Drugs targeting the ribosome. *Curr Opin Struct Biol* **15:**355–366.
Katz L and Ashley GW (2005) Translation and Protein synthesis: Macrolides. *Chem Rev* **105:**499–527.
Kirst HA, Debono M, Toth JE, Truedell BA, Willard KE, Ott JL, Counter FT, Felty-Duckworth AM, and Pekarek RS (1986) Synthesis and antimicrobial evaluation of acyl derivatives of 16-membered macrolide antibiotics related to tylosin. *J Antibiot (Tokyo)* **39:**1108–1122.
Lovmar M, Tenson T, and Ehrenberg M (2004) Kinetics of macrolide action: the josamycin and erythromycin cases. *J Biol Chem* **279:**53506–53515.
Morrison JF and Walsh C (1988) The behavior and significance of slow-binding inhibitors. *Adv Enzymol Relat Areas Mol Biol* **61:**201–301.
Omura S (2002) Macrolide antibiotics: chemistry, biology and practice. Academic Press, Orlando, FL.
Pestka S and Lemahieu RA (1974) Effect of erythromycin analogues on binding of [^{14}C]erythromycin to *Escherichia coli* ribosomes. *Antimicrob Agents Chemother* **6:**479–488.
Picking WD, Odom OW, Tsalkova T, Serdyuk I, and Hardesty B (1991) The conformation of nascent polylysine and polyphenylalanine peptides on ribosomes. *J Biol Chem* **266:**1534–1542.
Rheinberger HJ, Geigenmuller U, Wedde M, and Nierhaus KH (1988) Parameters for the preparation of *Escherichia coli* ribosomes and ribosomal subunits active in tRNA binding. *Methods Enzymol* **164:**658–670.
Seo HS, Abedin S, Kamp D, Wilson DN, Nierhaus KH, and Cooperman BS (2006) EF-G-Dependent GTPase on the ribosome. Conformational change and fusidic acid inhibition. *Biochemistry* **45:**2504–2514.
Schafer MA, Tastan AO, Patzke S, Blaha G, Spahn CM, Wilson DN, and Nierhaus KH (2002) Codon-anticodon interaction at the P site is a prerequisite for tRNA interaction in the small ribosomal subunit. *J Biol Chem* **277:**19095–19105.
Schloss JV (1988) Significance of slow-binding enzyme inhibition and its relationship to reaction-intermediate analogues. *Acc Chem Res* **21:**348–353.
Schlunzen F, Zarivach R, Harms J, Bashan A, Tocilj A, Albrecht R, Yonath A, and Franceschi F (2001) Structural basis for the interaction of antibiotics with the peptidyl transferase centre in eubacteria. *Nature (Lond)* **413:**814–821.
Stern S, Moazed D, and Noller H (1988) Structural analysis of RNA using chemical and enzymatic probing monitored by primer extention. *Methods Enzymol* **164:**481–489.
Triman K, Becker E, Dammel C, Katz J, Mori H, Douthwaite S, Yapijakis C, Yoast S, and Noller HF (1989) Isolation of temperature-sensitive mutans of 16S rRNA in *Escherichia coli*. *J Mol Biol* **209:**645–653.
Tu D, Blaha G, Moore PB, and Steitz TA (2005) Structures of MLSBK antibiotics bound to mutated large ribosomal subunits provide a structural explanation for resistance. *Cell* **121:**257–270.
Vester B and Douthwaite S (2001) Macrolide resistance conferred by base substitutions in 23S rRNA. *Antimicrob Agents Chemother* **45:**1–12.
Wilson DN, Harms JM, Nierhaus KH, Schlunzen F, and Fucini P (2005) Species-specific antibiotic-ribosome interactions: implications for drug development. *Biol Chem* **386:**1239–1252.
Xiong L, Shah S, Mauvais P, and Mankin AS (1999) A ketolide resistance mutation in domain II of 23S rRNA reveals the proximity of hairpin 35 to the peptidyl transferase centre. *Mol Microbiol* **31:**633–639.

Address correspondence to: George P. Dinos, Laboratory of Biochemistry, School of Medicine, University of Patras, 26500-Patras, Greece. E-mail: geodinos@med.upatras.gr